Optical circular polarization induced by axion-like particles in blazars

Runmin Yao

Institute of High Energy Physics, Chinese Academy of Sciences

In collaboration with
Xiaojun Bi, Jinwei Wang, Pengfei Yin

November 23, 2022

Contents

ALP-photon effects

Effective Lagrangian

$$\mathcal{L}_{\mathrm{a}\gamma\gamma} = -\frac{1}{4} g_{a\gamma}\, a F_{\mu\nu} \tilde{F}^{\mu\nu} = g_{a\gamma}\, a \boldsymbol{E} \cdot \boldsymbol{B} \tag{1}$$

ALP-photon effects

Effective Lagrangian

$$\mathcal{L}_{a\gamma\gamma} = -\frac{1}{4} g_{a\gamma} a F_{\mu\nu} \tilde{F}^{\mu\nu} = g_{a\gamma} a \boldsymbol{E} \cdot \boldsymbol{B} \tag{1}$$

Birefringence

Dispersion relation

$$\omega^2 - k^2 \approx \pm g_{a\gamma\gamma} (\omega \partial_z a + k \dot{a})$$

$$\Downarrow$$

Polarization rotation

$$\Delta\psi \approx \frac{1}{2} g_{a\gamma} \left[a(x_2, t_2) - a(x_1, t_1) \right]$$

ALP-photon effects

Effective Lagrangian

$$\mathcal{L}_{a\gamma\gamma} = -\frac{1}{4} g_{a\gamma} a F_{\mu\nu} \tilde{F}^{\mu\nu} = g_{a\gamma} a \boldsymbol{E} \cdot \boldsymbol{B} \tag{1}$$

Birefringence

Dispersion relation

$$\omega^2 - k^2 \approx \pm g_{a\gamma\gamma} (\omega \partial_z a + k \dot{a})$$

$$\Downarrow$$

Polarization rotation

$$\Delta\psi \approx \frac{1}{2} g_{a\gamma} \left[a(x_2, t_2) - a(x_1, t_1) \right]$$

Mixing

Conversion between the ALP and the photon polarization component that in parallel to the external magnetic field

- Spectra
- Polarization

ALP-photon mixing

Equation of motion

$$\left(i\frac{d}{dz} + E + \mathcal{M}\right)\psi(z) = 0, \tag{2}$$

with

$$\psi(z) = \begin{pmatrix} A_x(z) \\ A_y(z) \\ a(z) \end{pmatrix}, \ \mathcal{M} = V^{\dagger}(\phi)\mathcal{M}^{(0)}\,V(\phi). \tag{3}$$

Polarization density matrix

$$\rho(z) = \begin{pmatrix} A_x(z) \\ A_y(z) \\ a(z) \end{pmatrix} \otimes \begin{pmatrix} A_x(z) & A_y(z) & a(z) \end{pmatrix}^*, \tag{4}$$

which obeys the Liouville-Von Neumann equation

$$i\frac{d\rho}{dz} = [\rho, \mathcal{M}]. \tag{5}$$

Astrophysical sources

Mixing matrix

$$\mathcal{M}^{(0)} = \begin{pmatrix} \Delta_\perp & 0 & 0 \\ 0 & \Delta_\parallel & \Delta_{a\gamma} \\ 0 & \Delta_{a\gamma} & \Delta_a \end{pmatrix} , \tag{6}$$

$$\Delta_{a\gamma} \equiv \frac{1}{2} g_{a\gamma} B_{\rm T}, \quad \Delta_\perp \equiv \Delta_{\rm pl} + \Delta_{\rm abs} + \Delta_{\rm CMB} + 2\Delta_{\rm QED},$$

$$\Delta_a \equiv -\frac{m_a^2}{2E}, \quad \Delta_\parallel \equiv \Delta_{\rm pl} + \Delta_{\rm abs} + \Delta_{\rm CMB} + 3.5\Delta_{\rm QED}.$$

Astrophysical sources

Mixing matrix

$$\mathcal{M}^{(0)} = \begin{pmatrix} \Delta_\perp & 0 & 0 \\ 0 & \Delta_\parallel & \Delta_{a\gamma} \\ 0 & \Delta_{a\gamma} & \Delta_a \end{pmatrix} , \tag{6}$$

$$\Delta_{a\gamma} \equiv \frac{1}{2} g_{a\gamma} B_{\rm T}, \quad \Delta_\perp \equiv \Delta_{\rm pl} + \Delta_{\rm abs} + \Delta_{\rm CMB} + 2\Delta_{\rm QED},$$

$$\Delta_a \equiv -\frac{m_a^2}{2E}, \quad \Delta_\parallel \equiv \Delta_{\rm pl} + \Delta_{\rm abs} + \Delta_{\rm CMB} + 3.5\Delta_{\rm QED}.$$

- High energy photons

Astrophysical sources

Mixing matrix

$$\mathcal{M}^{(0)} = \begin{pmatrix} \Delta_\perp & 0 & 0 \\ 0 & \Delta_\parallel & \Delta_{a\gamma} \\ 0 & \Delta_{a\gamma} & \Delta_a \end{pmatrix} , \tag{6}$$

$$\Delta_{a\gamma} \equiv \frac{1}{2} g_{a\gamma} B_{\rm T}, \quad \Delta_\perp \equiv \Delta_{\rm pl} + \Delta_{\rm abs} + \Delta_{\rm CMB} + 2\Delta_{\rm QED},$$

$$\Delta_a \equiv -\frac{m_a^2}{2E}, \quad \Delta_\parallel \equiv \Delta_{\rm pl} + \Delta_{\rm abs} + \Delta_{\rm CMB} + 3.5\Delta_{\rm QED}.$$

- High energy photons
- Resonant conversion in strong magnetic fields

Astrophysical sources

Mixing matrix

$$\mathcal{M}^{(0)} = \begin{pmatrix} \Delta_\perp & 0 & 0 \\ 0 & \Delta_\parallel & \Delta_{a\gamma} \\ 0 & \Delta_{a\gamma} & \Delta_a \end{pmatrix} , \tag{6}$$

$$\Delta_{a\gamma} \equiv \frac{1}{2} g_{a\gamma} B_{\rm T}, \quad \Delta_\perp \equiv \Delta_{\rm pl} + \Delta_{\rm abs} + \Delta_{\rm CMB} + 2\Delta_{\rm QED},$$

$$\Delta_a \equiv -\frac{m_a^2}{2E}, \quad \Delta_\parallel \equiv \Delta_{\rm pl} + \Delta_{\rm abs} + \Delta_{\rm CMB} + 3.5\Delta_{\rm QED}.$$

- High energy photons
- Resonant conversion in strong magnetic fields
- Magnetic fields in large scales

Stokes parameters

$$\rho_\gamma = \frac{1}{2}\begin{pmatrix} I+Q & U-iV \\ U+iV & I-Q \end{pmatrix} \tag{7}$$

Stokes parameters

$$\rho_\gamma = \frac{1}{2}\begin{pmatrix} I+Q & U-iV \\ U+iV & I-Q \end{pmatrix} \tag{7}$$

- I: Intensity of photons
- $\Pi_{\rm L} \equiv \frac{\sqrt{Q^2+U^2}}{I}$: Degree of linear polarization
- $\Pi_{\rm C} \equiv \frac{V}{I}$: Degree of circular polarization

Stokes parameters

$$\rho_\gamma = \frac{1}{2}\begin{pmatrix} I+Q & U-iV \\ U+iV & I-Q \end{pmatrix} \tag{7}$$

- I: Intensity of photons
- $\Pi_{\rm L} \equiv \frac{\sqrt{Q^2+U^2}}{I}$: Degree of linear polarization
- $\Pi_{\rm C} \equiv \frac{V}{I}$: Degree of circular polarization

As for the numerical calculation of the astrophysical magnetic field, the field environment is sliced into N consecutive domains with homogeneous magnetic fields. For each domain, the EOM can be solved exactly. The photon state and Stokes parameters at any propagation distance can be obtained by iterating.

Optical circular polarization

Weak-mixing condition

$$|\Delta_{\rm pl}| \gg \Delta_{a\gamma},\ |\Delta_{\rm pl}| \gg |\Delta_a|. \tag{8}$$

In this regime, the conversion probability turns out to be vanishingly small. And the changes of I, Q, and U are negligible at first leading order.

Optical circular polarization

Weak-mixing condition

$$|\Delta_{\rm pl}| \gg \Delta_{a\gamma},\ |\Delta_{\rm pl}| \gg |\Delta_a|. \tag{8}$$

In this regime, the conversion probability turns out to be vanishingly small. And the changes of I, Q, and U are negligible at first leading order.

Circular polarization

$$\begin{aligned} V(z) &= V(z_0)\cos\kappa + \mathcal{V}\sin\kappa, \\ \mathcal{V} &\equiv Q(z_0)\sin 2\phi + U(z_0)\cos 2\phi, \\ \kappa &\equiv \left(\frac{\Delta_{a\gamma}^2}{\Delta_{\rm pl}} - \frac{1}{2}\Delta_a\right)(z - z_0)\ . \end{aligned} \tag{9}$$

Optical circular polarization

Single domain:

$$V(z) = V(z_0)\cos\kappa + \mathcal{V}\sin\kappa \tag{10}$$

Multi domains ($|\kappa| \ll 1$):

$$\begin{aligned} & V(z) - V(z_0) \\ \approx & \int_{z_0}^{z} \mathcal{V}\left(\frac{\Delta_{a\gamma}^2}{\Delta_{\rm pl}} - \frac{1}{2}\Delta_a\right) dz' \\ = & -\frac{m_e g_{a\gamma}^2 \mathcal{V} E}{8\pi\alpha}\int_{z_0}^{z}\frac{B_T^2(z')}{n_e(z')}dz' + \frac{m_a^2}{4E}\mathcal{V}(z-z_0). \end{aligned} \tag{11}$$

For linearly polarized photons,

$$\mathcal{V} = \Pi_{\rm L}\sin 2(\phi - \psi). \tag{12}$$

ϕ: Magnetic field angle
ψ: Polarization angle

Optical circular polarization

Single domain:

$$V(z) = V(z_0)\cos\kappa + \mathcal{V}\sin\kappa \tag{10}$$

Multi domains ($|\kappa| \ll 1$):

$$\begin{aligned} & V(z) - V(z_0) \\ \approx & \int_{z_0}^{z} \mathcal{V}\left(\frac{\Delta_{a\gamma}^2}{\Delta_{\rm pl}} - \frac{1}{2}\Delta_a\right) dz' \\ = & -\frac{m_e g_{a\gamma}^2 \mathcal{V} E}{8\pi\alpha}\int_{z_0}^{z} \frac{B_T^2(z')}{n_e(z')}dz' + \frac{m_a^2}{4E}\mathcal{V}(z-z_0). \end{aligned} \tag{11}$$

For linearly polarized photons,

$$\mathcal{V} = \Pi_{\rm L}\sin 2(\phi - \psi). \tag{12}$$

ϕ: Magnetic field angle
ψ: Polarization angle

BL lacs configuration

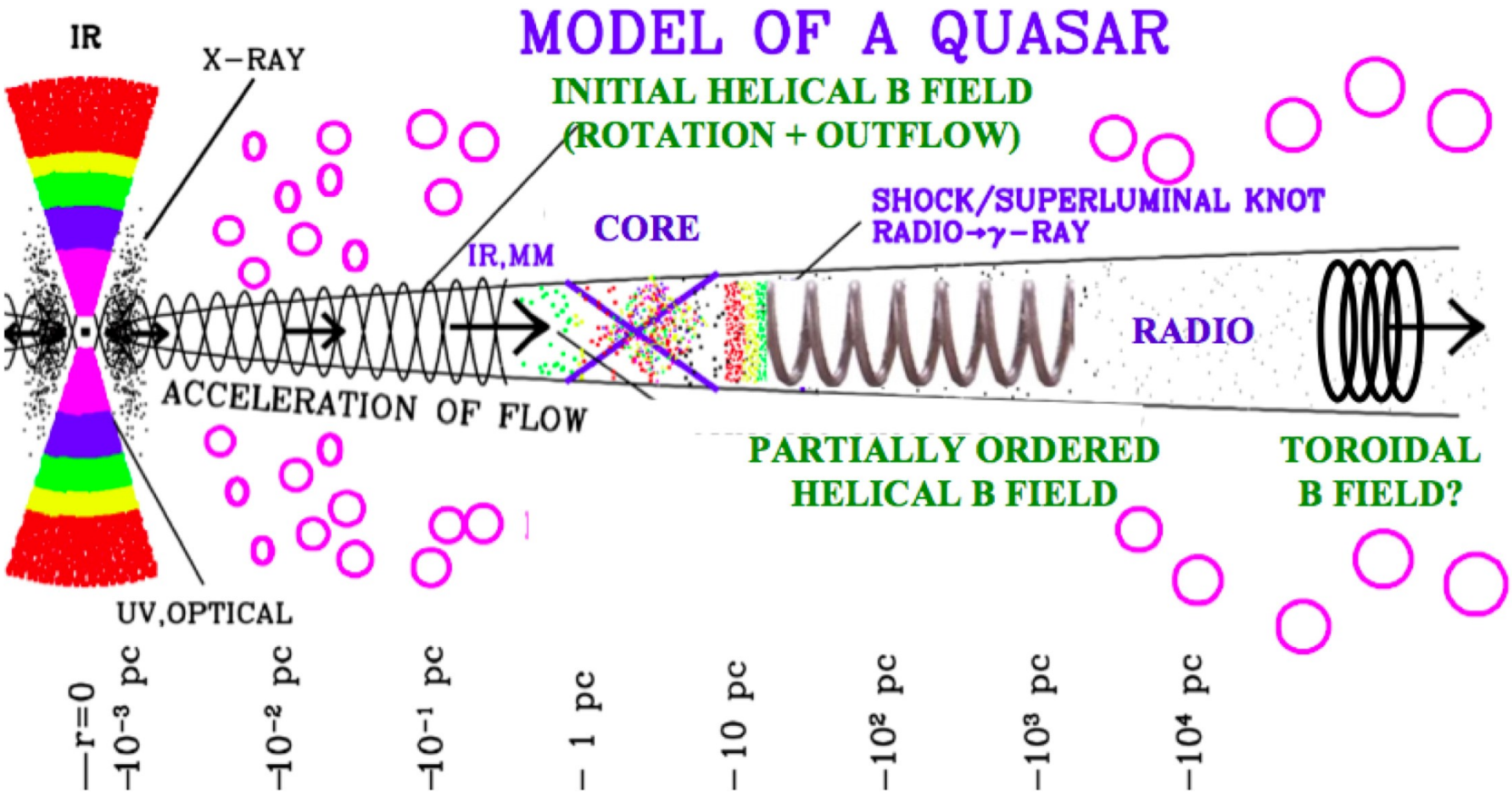

Figure 1: Jet Structure from Gabuzda, 2017

BL lacs configuration

The CP in optical emissions is hardly detected in blazars, while the degree of LP is typically at a level of $\sim 10\%$ and can be up to $\sim 50\%$ sometimes. Therefore, we can set constraint on the parameters of the ALP utilizing the CP effect.

BL lacs configuration

The CP in optical emissions is hardly detected in blazars, while the degree of LP is typically at a level of $\sim 10\%$ and can be up to $\sim 50\%$ sometimes. Therefore, we can set constraint on the parameters of the ALP utilizing the CP effect.

Field model

$$B_T^{\rm jet} = B_{T0}\left(\frac{r}{r_{\rm E}}\right)^{-1},\ n_e^{\rm jet} = n_{e0}\left(\frac{r}{r_{\rm E}}\right)^{-2} \tag{13}$$

- Co-moving frame
- $r_{\rm E}$: The distance of the emission site from the central black hole

Results

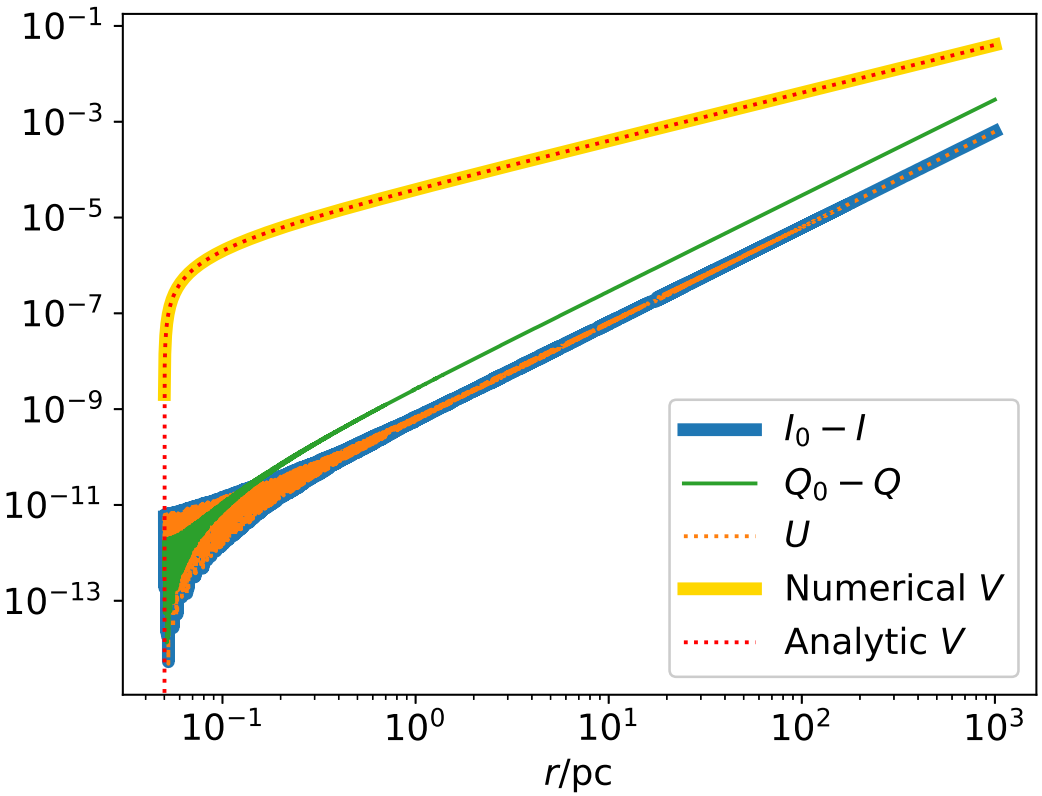

Figure 2: The evolution of Stokes parameters through the jet with the distance r.

Parameters:

$$r_{\rm E} = 0.05 \text{ pc}, \quad B_{T0} = 1 \text{ G}$$

$$n_{\rm e0} = 5 \times 10^4 \text{ cm}^{-3}$$

$$\Pi_L = 0.3, \quad \mathcal{V} = -\Pi_L$$

$$E' = 2 \text{ eV}, \quad \delta = 15.64$$

$$m_a = 10^{-15} \text{ eV}$$

$$g_{a\gamma} = 5 \times 10^{-11} \text{ GeV}^{-1}$$

Results

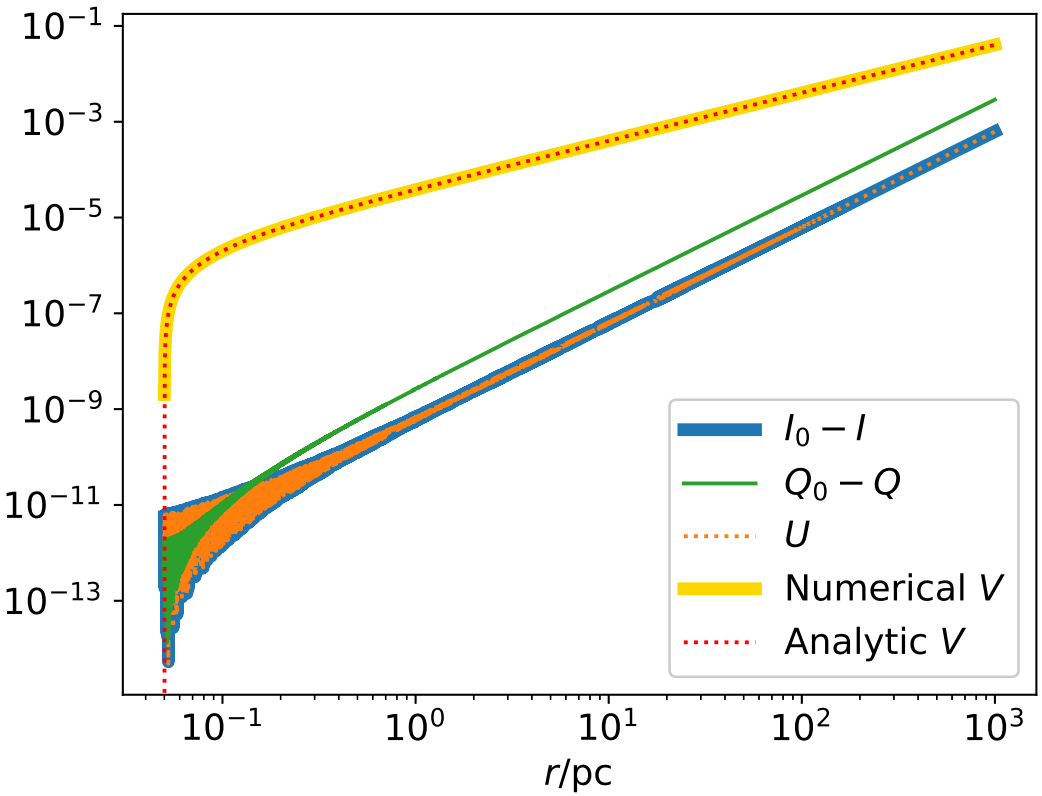

Figure 2: The evolution of Stokes parameters through the jet with the distance r.

Parameters:

$$r_{\rm E} = 0.05 \text{ pc}, \quad B_{T0} = 1 \text{ G}$$

$$n_{\rm e0} = 5 \times 10^4 \text{ cm}^{-3}$$

$$\Pi_L = 0.3, \quad \mathcal{V} = -\Pi_L$$

$$E' = 2 \text{ eV}, \quad \delta = 15.64$$

$$m_a = 10^{-15} \text{ eV}$$

$$g_{a\gamma} = 5 \times 10^{-11} \text{ GeV}^{-1}$$

ALPs can induce a much larger CP compared with LP. The analytic result of V is consistent with the numerical result.

Constraints

Hutsemekers et al., 2010 reported null detection of CP with typical uncertainties $< 0.1\%$ in 21 quasars except for two highly polarized blazars.

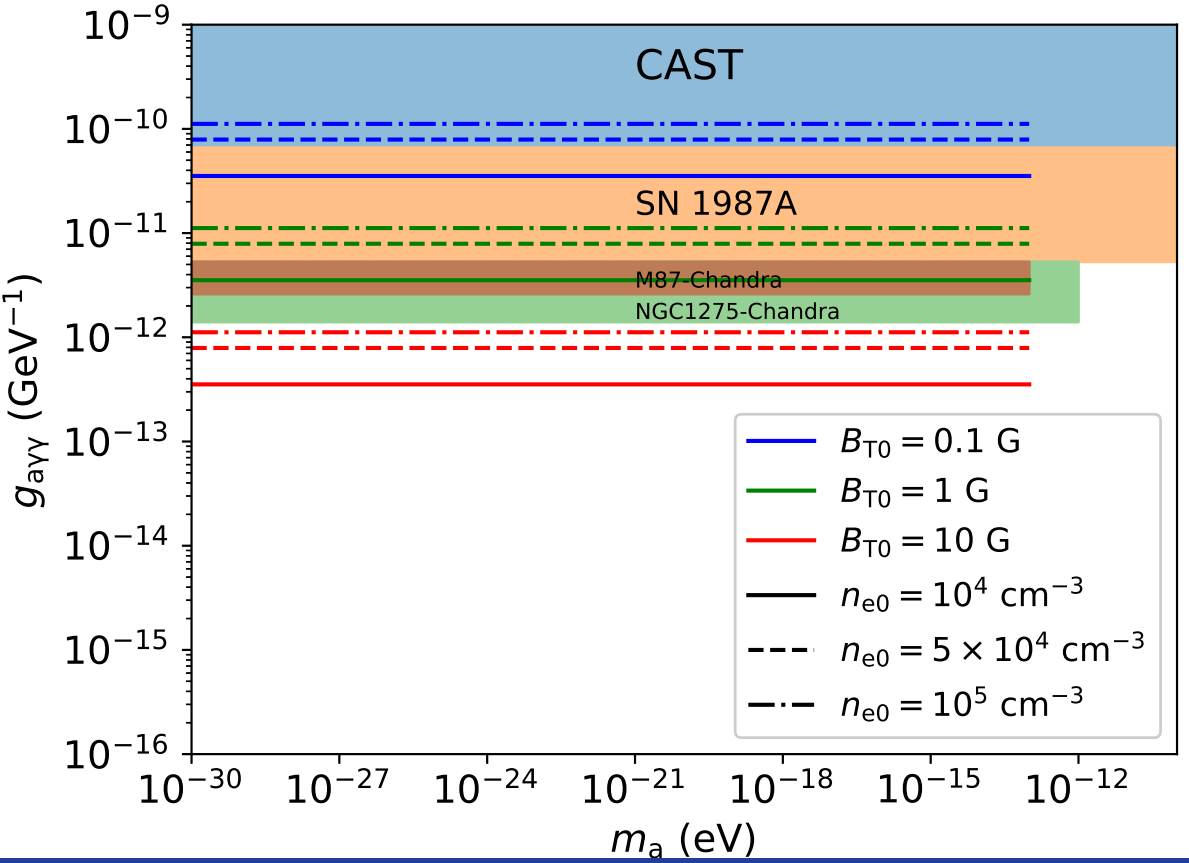

Figure 3: Bounds on the ALP-photon coupling in comparison to other bounds.(Anastassopoulos et al., 2017; Payez et al., 2015; Berg et al., 2017; Marsh et al., 2017)

Optical CP observation

Although the optical CP is rarely observed, there are some observations indicating CP detection.

- Small but significant optical CP in two blazars with uncertainties $< 0.1\%$. (Hutsemekers et al., 2010)
- A marginal detection of the optical CP at 2σ level in V and R bands for 3C 66A. (Tommasi, L. et al., 2001)
- A $3-6\sigma$ detection of CP with large values for 3C 66A. (Takalo and Sillanpaa, 1993)

Optical CP observation

Although the optical CP is rarely observed, there are some observations indicating CP detection.

- Small but significant optical CP in two blazars with uncertainties $< 0.1\%$. (Hutsemekers et al., 2010)
- A marginal detection of the optical CP at 2σ level in V and R bands for 3C 66A. (Tommasi, L. et al., 2001)
- A $3-6\sigma$ detection of CP with large values for 3C 66A. (Takalo and Sillanpaa, 1993)

These possible observations could be interpreted by the ALPs in the context.

Optical CP observation

Although the optical CP is rarely observed, there are some observations indicating CP detection.

- Small but significant optical CP in two blazars with uncertainties $< 0.1\%$. (Hutsemekers et al., 2010)
- A marginal detection of the optical CP at 2σ level in V and R bands for 3C 66A. (Tommasi, L. et al., 2001)
- A $3-6\sigma$ detection of CP with large values for 3C 66A. (Takalo and Sillanpaa, 1993)

These possible observations could be interpreted by the ALPs in the context.

Technique

Electron density distribution

$$n_{\rm e}(\gamma)=\begin{cases} n_{\rm e0}\gamma^{-p} & \text{for } 1\leqslant\gamma<\gamma_1 \\ n_{\rm e0}\gamma_1^{q-p}\gamma^{-q} & \text{for } \gamma_1\leqslant\gamma\leqslant\gamma_2 \\ 0 & \text{else} \end{cases}, \tag{14}$$

Assuming $B_{\rm T0}\approx B_0$,

$$\left(\frac{B_{T0}}{1\ \rm G}\right)^2\left(\frac{n_{\rm e0}}{5\times10^4\ \rm cm^{-3}}\right)^{-1}\approx\epsilon_{Be}f_\gamma \tag{15}$$

$$V(r)\propto g_{a\gamma}^2\Pi_{\rm L}\sin 2(\phi-\psi)E'\delta^{-1}\epsilon_{Be}f_\gamma r \tag{16}$$

When $\phi-\psi\approx k\pi/2\ \ (k\in\mathbb{Z})$,

$$\frac{\Pi_{\rm C}}{\Pi_{\rm L}E'}\propto g_{a\gamma}^2\epsilon_{Be}f_\gamma\delta^{-1}r_{\rm max}(\psi-\phi). \tag{17}$$

3C 66A

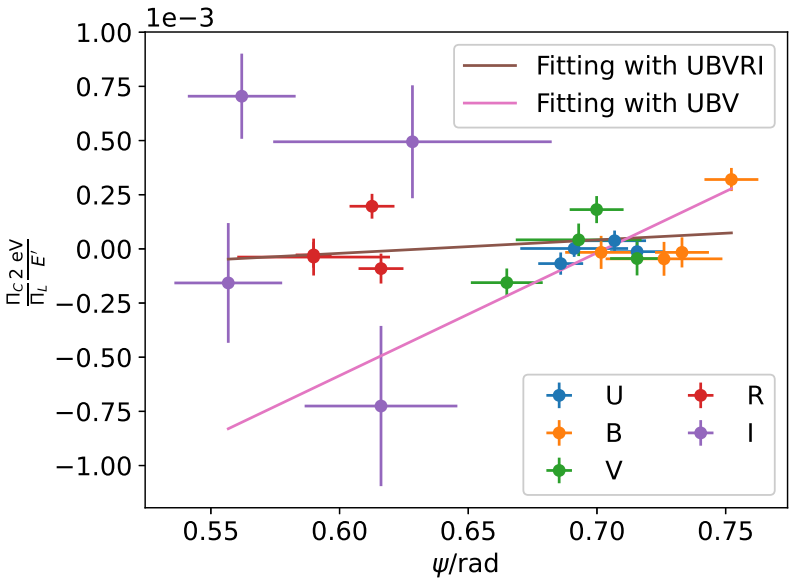

Bands	a_0	σ_{a_0}	a_1	σ_{a_1}
UBVRI	-0.39	0.45	0.62	0.66
UBV	-4.0	1.1	5.7	1.6

Table 1: Linear polynomial fit between the polarization angle ψ and $\frac{\Pi_C}{\Pi_L}\frac{2\ \mathrm{eV}}{E'}$,in the form of $y = a_0 + a_1 x$, using polarization observation data of 3C 66A in Takalo and Sillanpaa, 1993. Coefficients are in unit of 10^{-3}.

$$g_{a\gamma} \approx 7 \times 10^{-12}\ \mathrm{GeV}^{-1} \times \left[\epsilon_{Be} f_\gamma \left(\frac{15.64}{\delta}\right)\left(\frac{r_{\max}}{1\ \mathrm{kpc}}\right)\right]^{-1/2}. \quad (18)$$

3C 66A

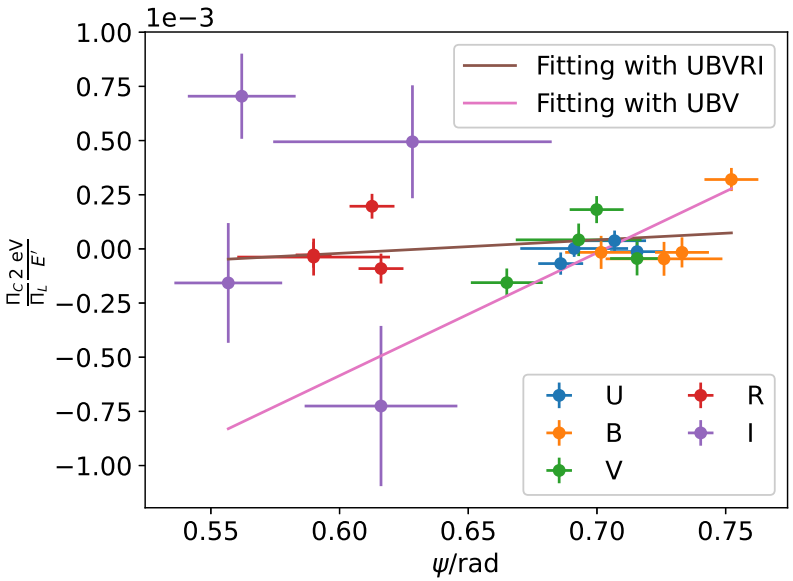

Bands	a_0	σ_{a_0}	a_1	σ_{a_1}
UBVRI	−0.39	0.45	0.62	0.66
UBV	−4.0	1.1	5.7	1.6

Table 1: Linear polynomial fit between the polarization angle ψ and $\frac{\Pi_C}{\Pi_L}\frac{2\ \mathrm{eV}}{E'}$,in the form of $y = a_0 + a_1 x$, using polarization observation data of 3C 66A in Takalo and Sillanpaa, 1993. Coefficients are in unit of 10^{-3}.

$$g_{a\gamma} \approx 7 \times 10^{-12}\ \mathrm{GeV}^{-1} \times \left[\epsilon_{Be} f_\gamma \left(\frac{15.64}{\delta}\right)\left(\frac{r_{\max}}{1\ \mathrm{kpc}}\right)\right]^{-1/2}. \quad (18)$$

SED Fit: $\delta \sim 30,\ f_\gamma \approx 1$

Different emission models:

- EC+SSC: $\epsilon_{Be} \sim 0.1$
  $\Rightarrow g_{a\gamma} \approx 3 \times 10^{-11}\ \mathrm{GeV}^{-1}$
- Pure SSC: $\epsilon_{Be} \sim 10^{-3}$
  $\Rightarrow$ Excluded
- Hadronic: $\epsilon_{Be} \sim 25$
  $\Rightarrow g_{a\gamma} \approx 2 \times 10^{-12}\ \mathrm{GeV}^{-1}$

OJ 287

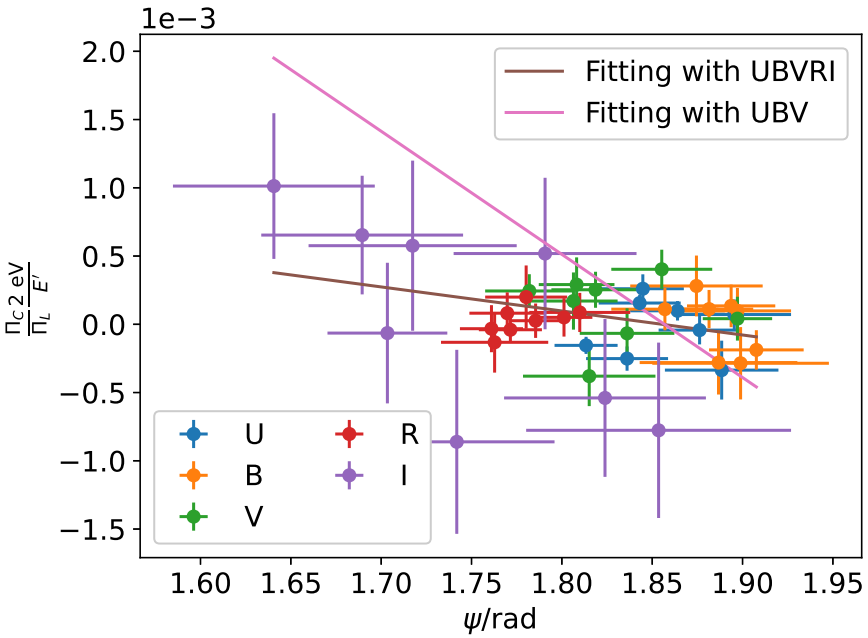

Bands	a_0	σ_{a_0}	a_1	σ_{a_1}
UBVRI	3.3	1.5	−1.8	0.79
UBV	16.8	6.4	−9.0	3.5

Table 2: Coefficients of linear polynomial fit to observation in OJ 287 in form of $\frac{\Pi_C}{\Pi_L}\frac{2\ eV}{E'} = a_0 + a_1\psi$. Parameters are in unit of 10^{-3}.

Bands	$\phi(rad)$	$g_{a\gamma}(10^{-12}\ \mathrm{GeV}^{-1})$	
		Leptonic	Hadronic
UBVRI	0.26 or 3.40	1.3	0.70
UBV	0.30 or 3.44	2.9	1.6

Table 3: Estimation of ϕ and $g_{a\gamma}$ using fitting coefficients in OJ 287. The factor $\sqrt{1\ \mathrm{kpc}/r_{\mathrm{max}}}$ in $g_{a\gamma}$ is omitted. $\delta = 15$. $f_\gamma \approx 1.2$, $\epsilon_{Be} = 8.2$ for leptonic model and $f_\gamma \approx 0.5$, $\epsilon_{Be} = 66$ for hadronic model (Boettcher et al., 2013).

Simultaneous LP and CP measurements in the optical band with high accuracy are needed to verify this analysis in the future.

More realistic case

It is worth noting that the above results are derived for the optimal case $\mathcal{V} = \pm\Pi_{\rm L}$, while the value of $\mathcal{V}$ is supposed to be smaller in the more realistic case.

Structure of Jet

- The direction of magnetic field could change during propagation and result in a shorter coherent length.
- The photons received by the detector are not from a certain point on the source but from the whole emitting region.

Other sources

- Intrinsic CP.
- The ALP-photon mixing in other astrophysical magnetic fields may contribute to the optical CP.

Partially random field

The direction of magnetic field is partially random in each calculation domain

$$\phi = \phi_0 + \alpha\Delta\phi, \quad \Delta\phi \in [-\pi, \pi) \tag{19}$$

The change of V

Given the approximation that $\alpha \ll 1$ is true,

$$\mathcal{V}_{n+1} \approx \Pi_L \sin 2(\phi_0 - \psi_n) + 2\alpha\Delta\phi_n \Pi_L \cos 2(\phi_0 - \psi_n), \tag{20}$$

- The incremental part: same as the idealized case
- The random part: random walk

Partially random field

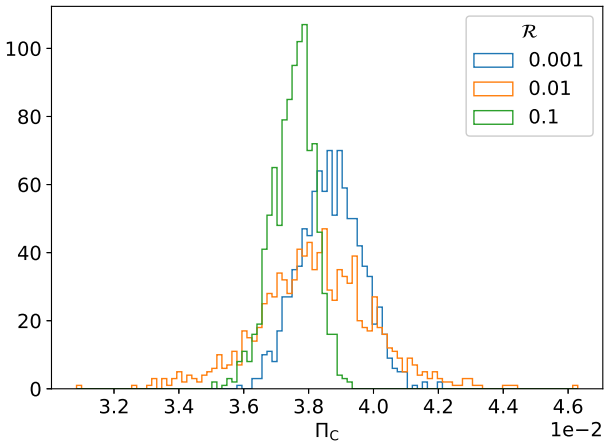

$\alpha = 0.1$

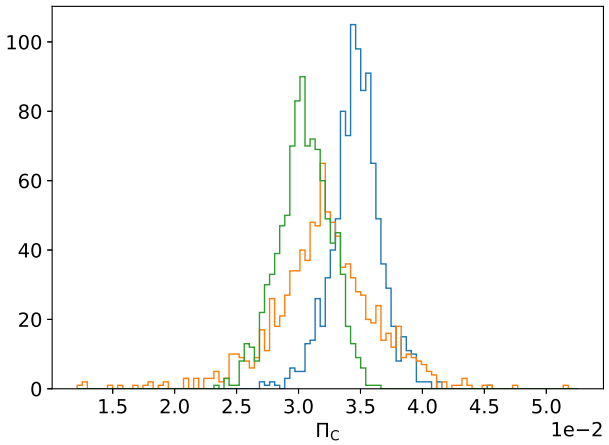

$\alpha = 0.2$

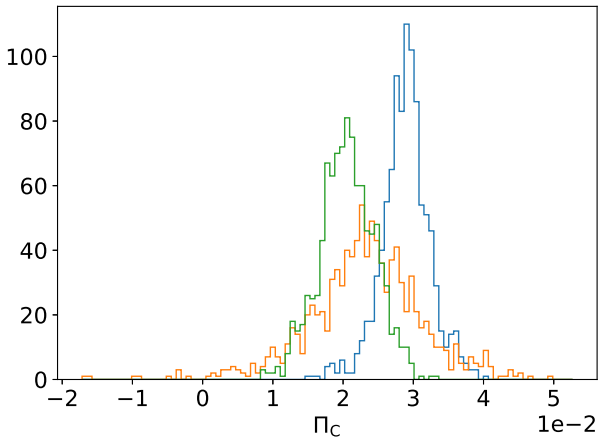

$\alpha = 0.3$

Figure 4: Distribution of optical CP induced by ALPs for magnetic field with varied angle in different cases. $\phi_0 = 3\pi/4$.

For a more realistic field configuration, the values of CP are smaller than the optimal case, while **its magnitude remains in the same order**.

Structure of jet

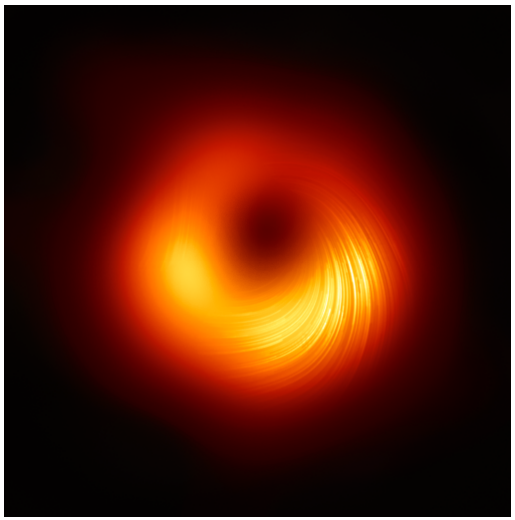

Figure 5: A view of the M87* supermassive black hole in polarised light, taken by Event Horizon Telescope.

The direction of the transverse magnetic field is spatial dependent. The density matrices of photons are calculated in multi paths, where Eq. (19) is still adopted but the values of ϕ_0 evenly vary in different paths. Then summing all density matrices, we obtain the assembly CP in a specific range of ϕ_0 in the numerical calculation.

Assembly CP

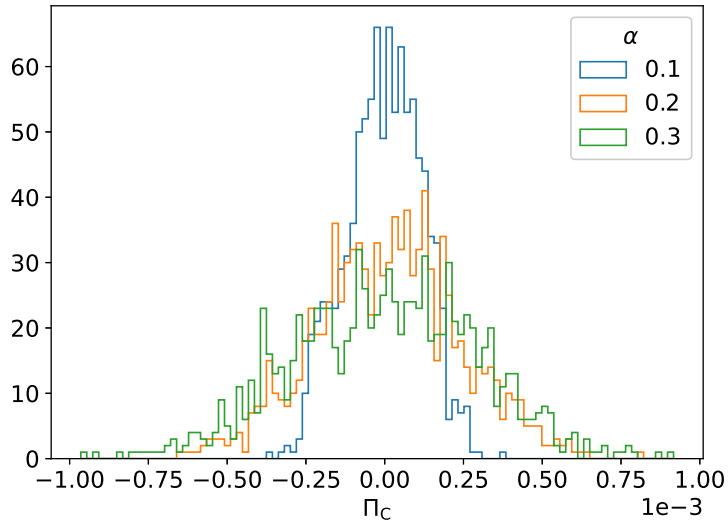

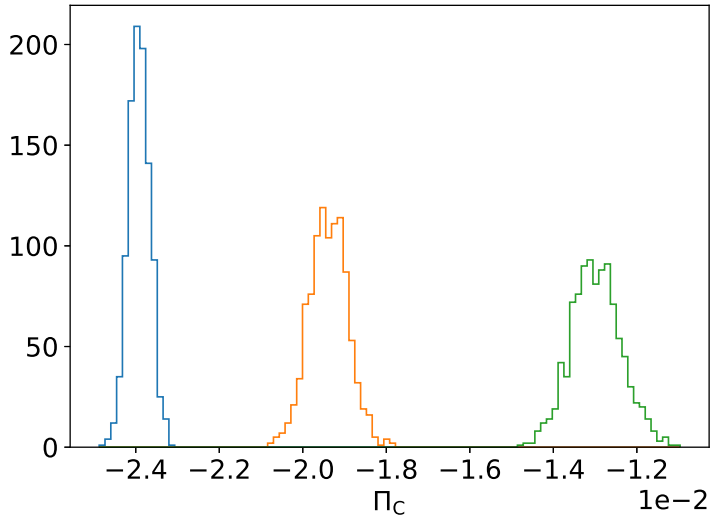

$\phi_0 : 0 \sim 2\pi$ $\phi_0 : 0 \sim \pi/2$

Figure 6: Distribution of assembly optical CP for partially random magnetic field with ϕ_0 in different intervals. The decrease ratio is chosen to be $\mathcal{R} = 0.1$ for simplicity.

High-precision measurements can help improve to observe the optical CP. Nevertheless, even in the low-precision cases, it is possible that there are some blazars that can produce observable CP.

Other astrophysical magnetic field

Mixing contribution to CP

$$V \sim \Pi_{\rm L} g_{a\gamma}^2 B^2 l_{\rm osc} L, \quad l_{\rm osc} = [(\Delta_a - \Delta_{\parallel})^2 + 4\Delta_{a\gamma}^2]^{-1/2} \tag{21}$$

Characteristic quantity

$$f_{\rm CP} \equiv \left(\frac{B}{1\ {\rm G}}\right)^2 \left(\frac{n_{\rm e}}{5\times 10^4\ {\rm cm}^{-3}}\right)^{-1} \left(\frac{L}{1\ {\rm kpc}}\right) \tag{22}$$

Scenarios	B(G)	$n_{\rm e}({\rm cm}^{-3})$	L(kpc)	$f_{\rm CP}$
Intra-cluster magnetic field	10^{-6}	10^{-3}	10	5×10^{-4}
Intergalactic magnetic field	10^{-9}	10^{-7}	5×10^4	2.5×10^{-2}
Galactic magnetic field	10^{-6}	10^{-1}	10^{-2}	5×10^{-9}

Table 4: The value of $f_{\rm CP}$ for different magnetic field scenarios.

The influence of other astrophysical magnetic fields can be neglected.

Summary

- ALP can induce optical CP in blazar.
- The measurement of CP can place constraints on ALP.
- Some possible observations of CP indicate the coupling $g_{a\gamma}$ to be the order of 10^{-12} GeV^{-1}.
- The partial random magnetic fields do not change the magnitude of ALP induced CP.
- High-precision measurements can help observe the optical CP.
- The influence of other astrophysical magnetic fields can be neglected.

Thanks!

References I

Anastassopoulos, V. et al. (2017). "New CAST Limit on the Axion-Photon Interaction". *Nature Phys.* 13, pp. 584–590. arXiv: 1705.02290 [hep-ex].

Berg, Marcus et al. (2017). "Constraints on Axion-Like Particles from X-ray Observations of NGC1275". *Astrophys. J.* 847.2, p. 101. arXiv: 1605.01043 [astro-ph.HE].

Boettcher, M. et al. (2013). "Leptonic and Hadronic Modeling of Fermi-Detected Blazars". *Astrophys. J.* 768, p. 54. arXiv: 1304.0605 [astro-ph.HE].

Gabuzda, Denise (Feb. 2017). "The Origin and Structure of the Magnetic Fields and Currents of AGN Jets". *Galaxies* 5.1, p. 11.

References II

Hutsemekers, D. et al. (2010). "Optical circular polarization in quasars". *Astron. Astrophys.* 520, p. L7. arXiv: 1009.4049 [astro-ph.CO].

Marsh, M. C. David et al. (2017). "A New Bound on Axion-Like Particles". *JCAP* 12, p. 036. arXiv: 1703.07354 [hep-ph].

Payez, Alexandre et al. (2015). "Revisiting the SN1987A gamma-ray limit on ultralight axion-like particles". *JCAP* 02, p. 006. arXiv: 1410.3747 [astro-ph.HE].

Takalo, Leo O. and Aimo Sillanpaa (Aug. 1993). "Simultaneous linear and circular polarization observations of blazars 3C 66A, OJ 287 and Markarian 421". *Astrophysics and Space Science* 206.2, pp. 191–196.

References III

Tommasi, L. et al. (2001). "Multiband optical polarimetry of BL Lacertae objects with the Nordic Optical Telescope ***". *A&A* 376.1, pp. 51–58.